Evidence for structural transformations in polymer melts

J. K. Krüger, L. Peetz and W. Wildner
Fachbereich Physik, Universität des Saarlandes, Bau 38, D-6600 Saarbrücken, W. Germany
and M. Pietralla
Abteilung Experimentelle Physik I, Universität Ulm, Oberer Eselsberg, D-7900 Ulm, W. Germany
(Received 16 July 1979)

Crystallizing and non-crystallizing polymers have been investigated by Brillouin spectroscopy in the liquid state. The temperature gradient of the sound velocity of crystallizing polymers shows a discontinuity at ~60–110K above the melting transition. The non-crystallizing polymers investigated show no uniform behaviour. We interpret the phase between the melt temperature and the temperature of the additional transformation as a phase of locally nematic structure. This interpretation is also supported by a study of density, refractive index, viscosity and hypersonic attenuation.

INTRODUCTION

The temperature gradient of the sound velocity of n-tetracosane melt has been shown to exhibit an unexpected discontinuity[1]. The temperature at this discontinuity agrees well with that found from a step in the magnetic susceptibility[2] of the same paraffin sample. Since structural transformations in condensed matter are often connected to an anomalous elastic behaviour, Brillouin spectroscopy (BS) provides a sensitive method of studying static and dynamic properties of the transition[3,4]. In the case of polymers it has been found that the quasistatic glass transition can be identified precisely through the BS method even in partly crystalline systems[5] and that changes in the microscopic structure are reflected by the measured frequency shifts.

Here we discuss whether the suspected local ordering of the paraffin melt is a general property of macromolecular melts. Such local ordering has been proposed by several authors[6–8] and is set out in detail in ref 9. However, up to this time it has not been clear whether ordering arises spontaneously in the sense of a phase transformation or not. We have studied the hypersonic properties of the following polymers: n-tetracosane ($C_{24}H_{50}$, TC); low molecular weight linear polyethylene (PE 6600, $\bar{M}_w$ = 6600); poly[4-methylpentene-1] (P4MP1)*; poly(trimethylhexamethyleneterephthalamide) (PA6-3-T)†, and atactic polystyrene (PS). P4MP1 is a partly crystalline, transparent polymer at room temperature[10]; PA6-3-T is an amorphous transparent polyamide[11]. With the exception of PA6-3-T all these materials show a step in the temperature coefficient of the hypersonic velocity at well-defined temperatures within the investigated temperature region.

EXPERIMENTAL

The spectrometer system as described elsewhere[5] was modified by the automated data acquisition and stabilization system DAS-1 from Burleigh Instruments[12]. Overloading of the photomultiplier tube by strong 'central' line elastic scattering was eliminated by amplitude modulation of the laser light by a Pockels cell. This cell was driven by logical signals from the segmented timebase of the DAS-1 system, a high voltage amplifier and a buffer amplifier, to protect the DAS-1 system. Thus, the Pockels cell was always perfectly synchronized with the segmented timebase of the DAS-1 system.

The high temperature measurements (up to 620K) were performed in an optical thermostat made in our laboratory. The temperature could be stabilized within an accuracy of ~0.1K, and was measured by calibrated thermocouples.

TC, PE6600 and P4MP1 were poured as powders into a thinfilm cuvette (Duran, 300 μm film thickness) and subsequently melted in a helium atmosphere to produce homogeneous planar samples. The cuvettes can be filled only with sufficiently fluid melts. In some cases the desired fluidity could only be achieved at rather high temperatures where the polymers began to degrade. This occurred for PE and therefore the degraded PE was characterized prior to the Brillouin measurements. Several samples had been prepared by the same procedure, and one of them was used in g.p.c. measurements. The resulting molecular weight distribution is shown in *Figure 1* giving a weight-average molecular weight $\bar{M}_w$ = 6600 with $\bar{M}_w/\bar{M}_n$ = 2. The P4MP1 samples giving curves B and C in *Figure 2* were probably also degraded to some extent. To reduce the filling temperature, samples of PS and P4MP1 (*Figure 2*) were prepared by pushing the melt with a piston into the cuvette‡. To minimize errors introduced by degradation during the Brillouin experiments, the first measurement was taken at the highest temperature. The accumulation time at each temperature was about 1 min. A new temperature was then set and measurements taken when temperature of the sample had been constant within 0.1K for 3 min. The temperature was measured by thermocouples within the melts. In order to control possible degradation and hysteresis effects, at least two temperature runs were performed for each polymer, except PA6-3-T. No devia-

* Trade name TPX, kindly supplied by Mitsui Petrochemical Inc. Ltd, Japan

† Trade name Trogamid T, kindly supplied by Dynamit Nobel AG, Troisdorf

‡ This filling procedure was performed by Dr. Münstedt at the BASF, Ludwigshafen

0032-3861/80/060620-07$02.00

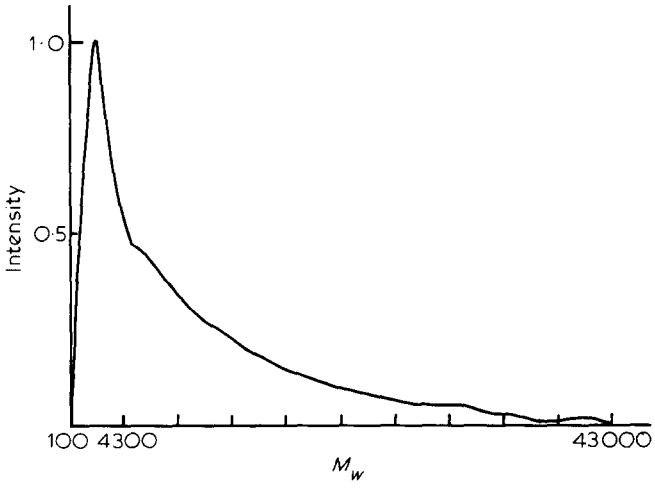

Figure 1 Molecular weight distribution of PE6600 as measured by g.p.c. $\bar{M}_w = 6600$; $\bar{M}_w/\bar{M}_n = 2$

tions exceeding the experimental accuracy were observed. A complete data set, including measurements at different wavelengths can be found in ref 1 for a sample of TC.

For the Brillouin-experiments we used the so called 90A and 90N scattering geometries[5]. The resulting sound velocities are given by:

$$90A \quad v_A(T) = f_A(T)\left[\frac{\lambda}{2n_a \sin(45°)}\right] \tag{1}$$

$$90N \quad v_N(T) = f_N(T)\left[\frac{\lambda}{2n(T)\sin(45°)}\right] \tag{2}$$

where v = sound velocity; T = temperature; f = phonon frequency; λ = wavelength of the laser light in vacuo; n = refractive index of the sample; and n_a = refractive index of the medium surrounding the sample. (in our experiments $n_a = 1$).

If no dispersion occurs, i.e. $v_A(T) = v_N(T)$, and $n_a = 1$, the temperature-dependent refractive index of the sample can be determined from the frequency shifts, f_A and f_N, of the two scattering geometries (equations 1,2) by $n(T) = f_N/f_A$. The 90A-geometry directly yields the sound velocity at constant phonon wavevector. The absolute accuracy for the sound frequencies f_A and f_N is estimated to be ~1%.

The sound attenuation can be derived from linewidth measurements. For this purpose we have digitally convoluted the line profile of a damped harmonic oscillator with the measured instrumental profile and compared it with the Brillouin-line profile. The Brillouin-linewidth (full width at half maximum) Δf is related to the hypersonic attenuation coefficient (spatial intensity decay) by:

$$\alpha = 2\pi\Delta f/v \tag{3}$$

The damped oscillator model is in good agreement with the measured line profiles.

For those cases where the data sets can be represented by two straight intersecting lines of the type:

$$g(T) = g(T_u)\,[1 - \delta(T - T_u)] \tag{4}$$

we use the following equation:

$$g(T) = a - bT \mp c|T - T_u| \tag{5}$$

to obtain a least squares fit. Thus all parameters, including the intersection temperature, are simultaneously determined. The discontinuous step in the temperature gradient is given by $2c$.

RESULTS

P4MP1

Figure 2a shows the hypersonic behaviour around the melt transition. Curve A was taken from a virgin sample. After subsequent heat treatment (used to fit the sample into a cuvette) the sample had clearly degraded to some extent and the sound velocity curve B shifted to lower sound

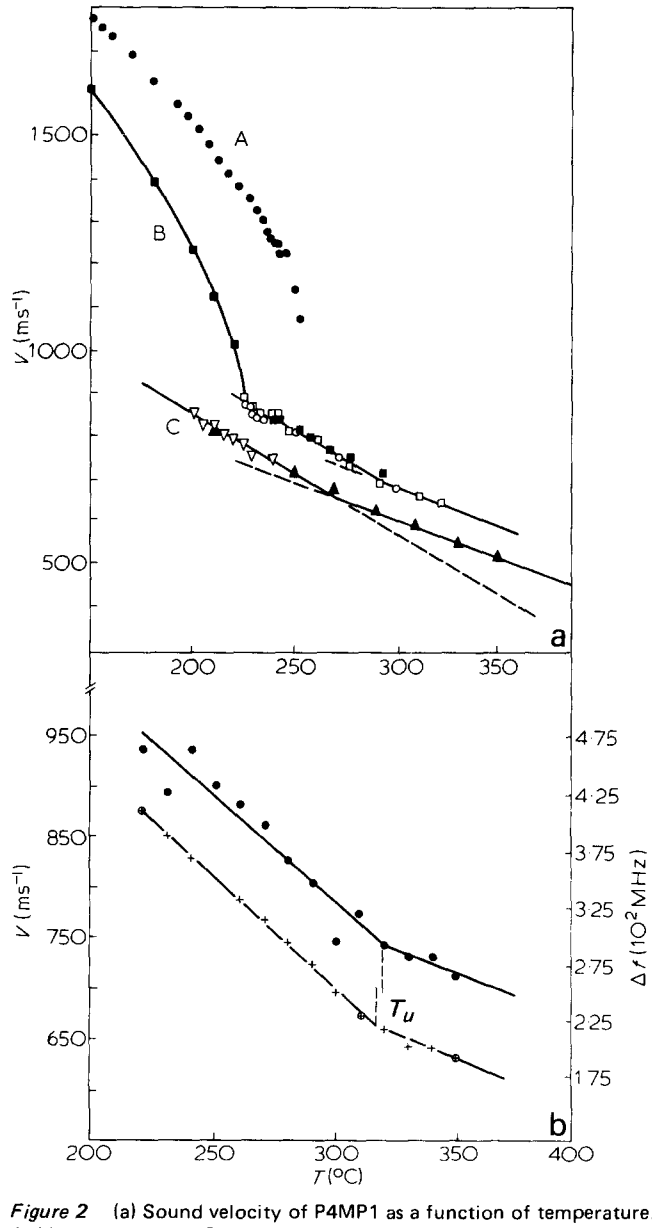

Figure 2 (a) Sound velocity of P4MP1 as a function of temperature. A, Virgin sample; B, C, measured on different runs with cuvettes filled at different temperatures. ▲○, First run; □, ▽, second run; ■, third run, (b) Sound velocity v (○, +) and sound attenuation Δf(●) of P4MP1 as a function of temperature T; T_u = transition temperature; +, first run, ○, second run

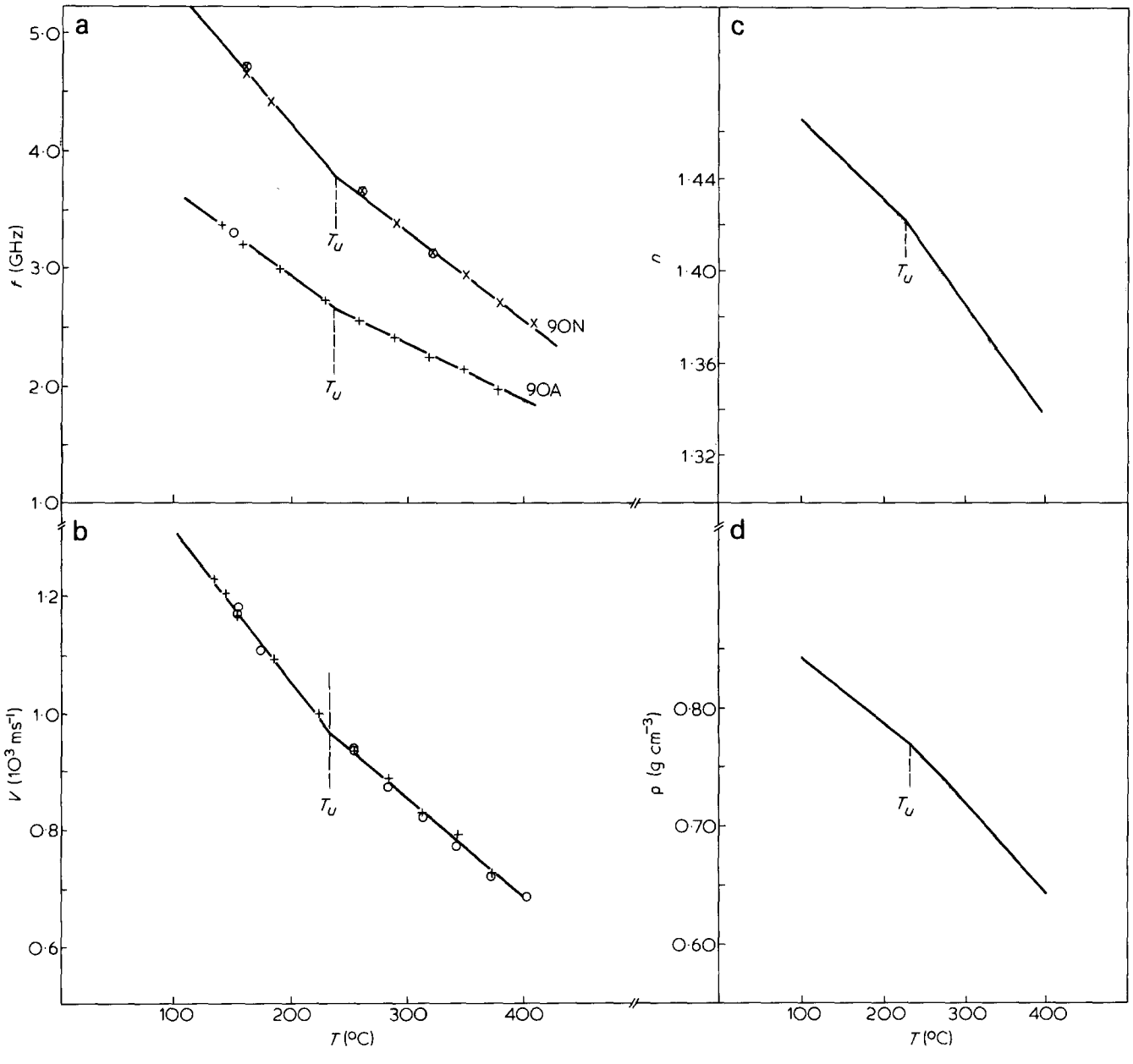

Figure 3 Brillouin investigations of PE6600. (a) Brillouin frequency shifts f in 90N and 90A scattering geometries as a function of temperature T. +, x, First run, ○, second run. (b) Sound velocity v *versus* temperature, T; +, from 90A; ○, indirectly from 90N. (c) Temperature dependent refractive index $n = n(T)$. (d) Temperature dependent density $\rho = \rho(T)$

velocities and the melting temperature decreased. Further degradation of the sample yielded curve C. Just below the maximum melting temperature, P4MP1 becomes completely opaque, preventing Brillouin measurements in this region. The origin of this 'critical opalescence' is not yet clear, but was also observed in polyisoprene at the melting point[13]. Well above the maximum melting temperature the sound velocity curves of samples B and C show kinks at 265° and 285°C, respectively. In order to ascertain the existence of the kink in the P4MP1 melt we repeated our measurements improving the spectrometer resolution and avoiding degradation effects during the sample preparation (see above). The result is shown in *Figure 2b*. By the fitting of the experimental data to equation (5) we can derive T_u and the temperature coefficient of the sound velocity below and above T_u according to equation (4) (*Table 1*). Within the accuracy of the experiment, hysteresis effects were not observed. The hypersonic attenuation of P4MP1 was also investigated (*Figure 2b*). Within an experimental error of about 10%, the data could be fitted by equation (5).

PE 6600

The sound frequencies of PE 6600 were determined in the temperature interval (130°–390°C) for the two scattering geometries 90A and 90N (see *Figure 3a*). As discussed above the sound velocity is determined by the 90A-sound frequencies (*Figure 3b*). As in the case of P4MP1 the data set can be well fitted to equation (5), (see *Table 1*). Because of the good linearity of the frequency curve (*Figure 3a*, 90A) above and below T_u, we conclude that there is no dispersion in this frequency region. If we assume a linear temperature dependence of the refractive index below and above T_u, the refractive index can be determined from the Brillouin data as a function of temperature (*Figure 3c*) (see above).

According to the Lorentz–Lorenz relation

$$(n^2 - 1)/(n^2 + 2) = r\rho \qquad (6)$$

Table 1 Physical properties of the polymers investigated

	T_U (°C)	$v(T_U)$ (ms^{-1})	$\delta_\perp$ (1/K) $\delta_\parallel$ (1/K)	$\rho(T_U)$:(g cm^{-3})	$\alpha'_\perp$ (1/K) $\alpha'_\parallel$ (1/K)	$n(T_U)$	$\beta_\perp$ (1/K) $\beta_\parallel$ (1/K)	$\gamma_\perp$ $\gamma_\parallel$
PE6600	230	966	2.68×10^{-3} 1.76×10^{-3}	0.769	7.40×10^{-4} 9.49×10^{-4}	1.4189	2.49×10^{-4} 3.20×10^{-4}	3.62 1.85
				$\Delta f(T_U)$ (MHz)	$\mu_\perp$ (1/K) $\mu_\parallel$ (1/K)	$E_\perp$ (kJ mol^{-1}) $E_\parallel$ (kJ mol^{-1})	$E_{o\perp}$ (kJ mol^{-1}) $E_{o\parallel}$ (kJ mol^{-1})	
P4MP1	316	658	3.43×10^{-3} 1.51×10^{-3}	301	$9.59\ 10^{-3}$ $2.82\ 10^{-3}$			
TC ($C_{24}H_{50}$)	110	1073	3.02×10^{-3} 2.43×10^{-3}	154	$2.74\ 10^{-2}$ $3.97\ 10^{-3}$	16.6 13.7	9.8 8.1	
				T_g (°C)	$v_l(T_g)$ (ms^{-1})	$\delta_\perp$ (1/K) $\delta_\parallel$ (1/K)	$v_t(T_g)$ (ms^{-1})	$\delta_\perp$ (1/K) $\delta_\parallel$ (1/K)
PS	273	1206	5.30×10^{-3} 3.70×10^{-3}	97	2339	1.01×10^{-3} 2.78×10^{-3}		
PA6-3-T				144.5	2457	9.52×10^{-4} 2.76×10^{-3}	1110	1.430×10^{-3} 4.80×10^{-3}

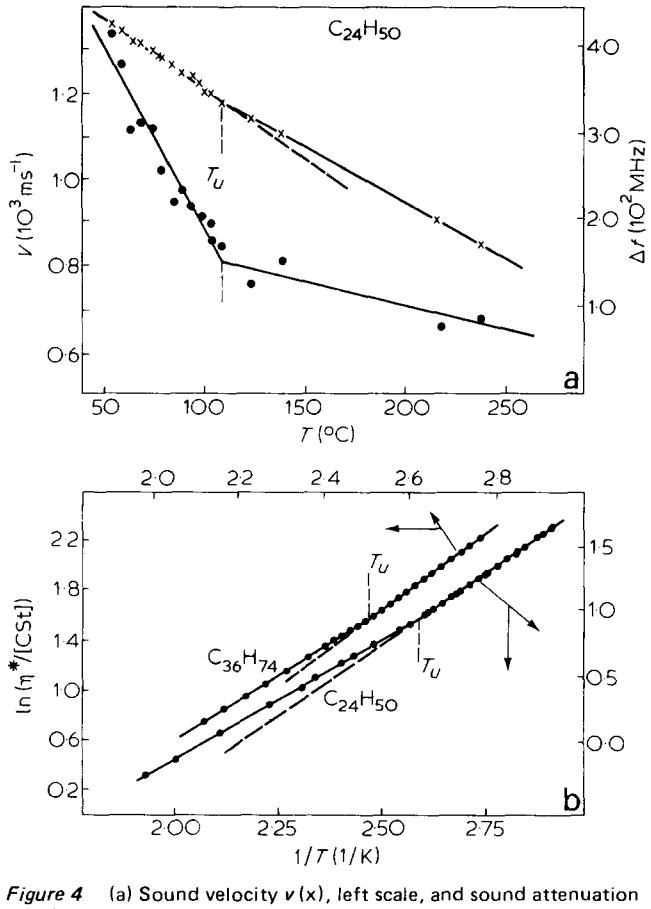

Figure 4 (a) Sound velocity v (x), left scale, and sound attenuation Δf (●), right scale, of TC as a function of temperature T; T_U = transition temperature. (b) Logarithm of the kinematic viscosity (lnη^*) of TC and $C_{36}H_{74}$ *versus* the inverse temperature ($1/T$); T_U = transition temperature

where n is the refractive index; r is the specific refractivity; and ρ is the density, we can also determine the temperature dependence of the density. The temperature dependence of the density can be described above and below T_u for linear PE, using a value $r = 0.3284$ cm^3 g^{-1} in the equation:

$$\rho(T) = \rho(T_u)\,[1 - \alpha'(T - T_u)] \qquad (7)$$

from which the volume expansion coefficient α' can be derived (see *Table 1*). From equation (7) the density of the amorphous structure at 25°C is found to be 0.886 g cm^{-3} which should be compared with 0.855 from the literature[14,15]. The difference is well within the range of experimental accuracy since the absolute value determined by equation (6) enhances the absolute value of the error given by the frequency measurement (1%) to about 5%. The relative accuracy of the temperature dependence should be better than 1%.

$C_{24}H_{50}$(TC) and $C_{36}H_{74}$(HTC)

Sound velocity data for the TC melt have previously been reported[1]. *Figure 4a* shows the sound velocity together with the related sound attenuation plotted against temperature for some of the data. The attenuation depends linearly on temperature above and below T_u, which is found to be 110°C – the same value as found from the sound velocity curve. The viscous behaviour of the TC and HTC melt has also been studied. An Ubbelohde viscosimeter was used to determine the kinematic viscosity η^* (*Figure 4b*). The temperature-dependent kinematic viscosity follows an exponential relationship above and below T_u:

$$\eta^* = C\exp(E/kT) \qquad (8)$$

where E is an activation energy for viscous flow and C is almost independent of temperature[15] (see below). The activation energies below and above T_u are different, and T_u = 110°C is in good agreement with the value found in the Brillouin-measurements. For HTC a value of T_u = 123.5°C is found.

PA6-3-T

Temperature-dependent Brillouin data of PA6-3-T are reported in *Figure 5*. The glass transition temperature T_g is found from the longitudinal as well as from the transverse phonon to be 144.5°C, which differes only slightly from T_g = 149°C found in literature[11]. Up to the highest temperature reached, 'the sound velocity–temperature curve shows no deviation from linear behaviour within an experimental error of about 1%.

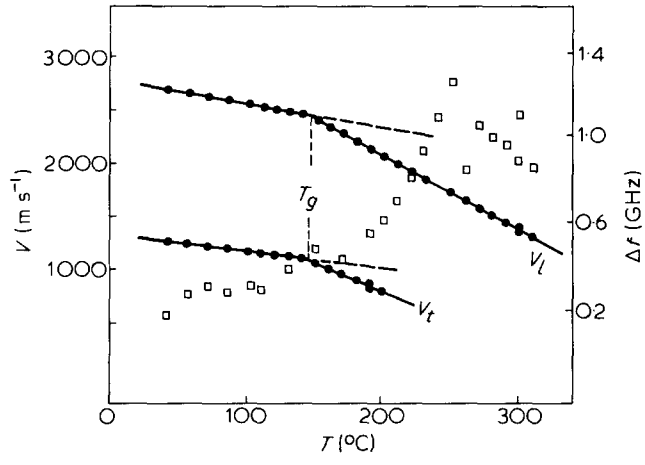

Figure 5 Longitudinal sound velocity v_1, transverse sound velocity v_t and the sound attenuation coefficient Δf of PA6-3-T *versus* temperature T; T_g = glass transition temperature

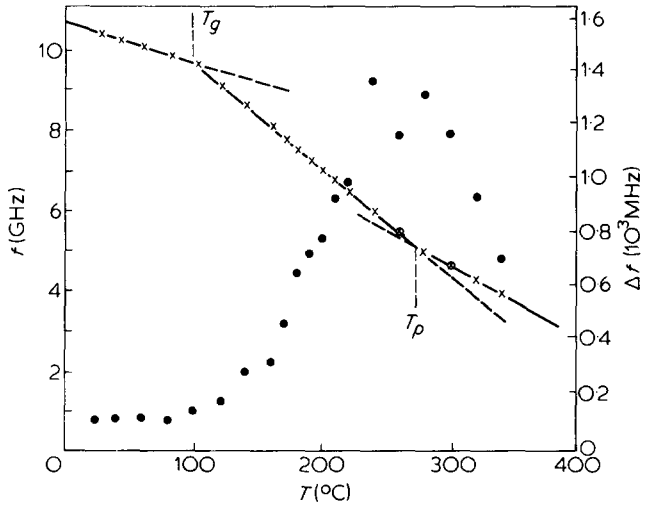

Figure 6 Sound velocity v(○, x), left scale, and sound attenuation, Δf(●), right scale, of PS *versus* temperature T; T_g = glass transition temperature; T_p = transition temperature; x, ●, first run; ○, second run

PS

PS has previously been investigated by Brillouin scattering, especially in the vicinity of the glass transition[16,17]. Patterson has measured the sound frequency and the sound attenuation above the glass transition of PS samples with different molecular weights[18]. The results are similar to ours, but the data are interpreted as a pure relaxational process, without any kink in the sound frequency curve.

We find a rather sharp kink at $T_p = 273°C$ in the sound frequency–temperature curve (*Figure 6*) above the glass transition temperature. The maximum in the sound attenuation data coincides with the kink in the sound frequency curve. *Figure 7* shows that we were also able to detect transverse phonons in PS not yet reported in literature.

DISCUSSION

If different physical properties of a system change abruptly by kinks or discontinuities at the same temperature, this can be an indication of a cooperative change of structure in the system. We have found this behaviour for the same physical properties of different polymer melts. We believe that an unexpected spontaneous change of structure appears in the melt of some polymers at a transition temperature T_u. We assume the phase above T_u to be isotropic (random coil) and below T_u to be at least of local nematic structure. Such local structures have already been discussed in the literature[1,2,7,19,26].

Since the idea of a cooperative transformation at T_u is based on the existence of a kink in the $v_s(T)$, $\Delta f(T)$ and $\ln\eta^*(1/T)$ curves we will outline the method of data analysis supporting the choice of equation (5). Besides the usual criteria (sum of least squares and the correlation matrix) we used the phase frequency test of Wallis and Moore[23] with the same conditions as in ref 24. This test analyses the distribution of subsequent data points around a given function and results in the randomness parameter Z. The data series can be regarded as random if $Z < Z_{crit}$ holds with $Z_{crit} = 1.96$[24]. Generally for our data sets presented here $Z < 1.5$. In addition, the lower bound of the correlation coefficients r^2 is 0.95 and in most cases even $r^2 > 0.99$ holds. Thus the choice of two straight intersecting lines provides a relevant description of our data sets.

All the partly crystalline polymers investigated (TC, P4MP1, PE6600) exhibit similar hypersonic properties in the melt region (*Table 1*).

(a) They show a kink in the sound velocity at T_u far above the melt transition temperature.

(b) The sound velocity changes linearly over wide temperature intervals above and below T_u.

(c) As expected, the temperature coefficient of the sound velocity is negative for both phases, but surprisingly the absolute value is larger in the low temperature phase.

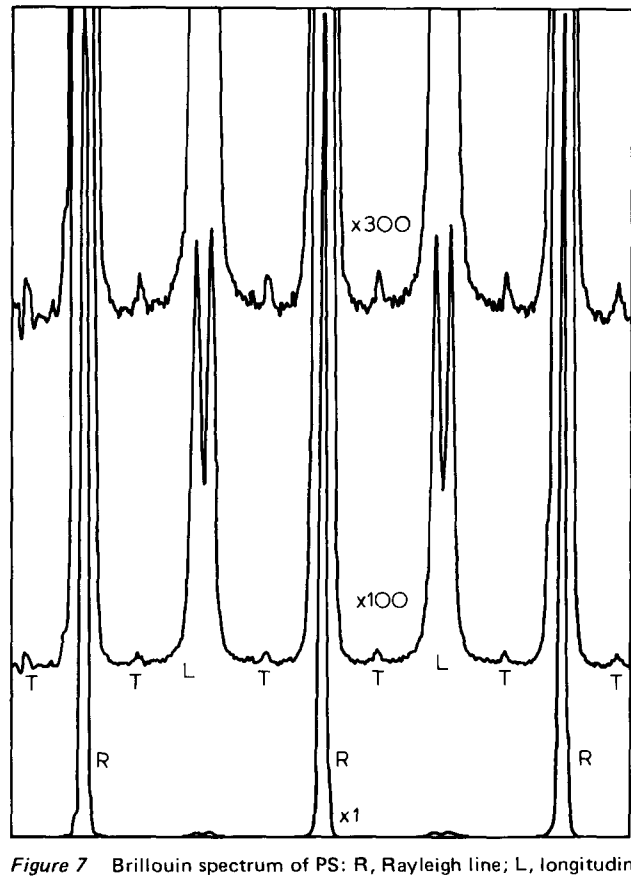

Figure 7 Brillouin spectrum of PS: R, Rayleigh line; L, longitudinal phonons; T, transverse phonons

(d) The hypersonic attenuation was investigated only in TC and P4MP1; it exhibits the same features as the sound velocity with nearly the same transition temperature.

(e) For PE6600, different scattering geometries were used to deduce the temperature dependence of the density and of the refractive index; both properties indicate the same transition temperature found in the sound velocity and attenuation measurements. The temperature coefficient of the refractive index and the volume expansion coefficient show finite discontinuities. The volume expansion coefficient of the low temperature phase is smaller than that of the high temperature phase. A simple Grüneisen evaluation with a single Grüneisen parameter has been used in literature to explain the elastic behaviour of PS at the glass transition[16] as well as for the elastic behaviour of the TC melt around T_u[1]:

$$\delta = \alpha' \gamma_i \tag{9}$$

γ_i is the Grüneisen number of the sound wavelength λ_i. The subscript i is preserved even though the sound frequency changes with temperature because the sound wavelength does not change. δ is the temperature coefficient of the sound velocity. For PE6600 such a simple Grüneisen-evaluation breaks down at T_u and two different Grüneisen parameters can be determined below and above T_u:

$$\gamma_{T \leqslant T_u} = 3.62$$

$$\gamma_{T > T_u} = 1.85$$

This may indicate that the molecular interaction forces change drastically from above to below T_u.

A transition from an isotropic to a locally nematic state at T_u is supported by the ultrasonic behaviour of low molecular weight liquid crystals at the isotropic–nematic transition[20,27–29]. For low frequencies, the sound velocity and the sound attenuation show relaxational behaviour near T_c. However, at frequencies higher than 115 MHz for PCB[28] and 23 MHz for MBBA[27] no relaxational behaviour is found for the sound velocity which only retains a small discontinuity at T_c. From *Figure 1* of ref 27 it is seen that at high frequencies the slopes of the sound velocity curves above and below T_c differ in a manner similar to their variation above and below T_u. In addition, the i.r. sound attentuation curves (*Figures 2* and *3* of ref 27) are similar to ours.

Below T_c and at high frequencies the hydrodynamic part of the sound attenuation increases more strongly with temperature than above T_c. The assumption of a damped harmonic oscillator model for the sound attenuation (equation 3) seems to be reasonable. Brillouin measurements on liquid crystals near T_c are controversial. Durand[30] found a dip in T_c in the sound attenuation of CEC at the isotropic–cholestric transition. Wang and Huang[31] found no anomaly at all in the data for CP at the isotropic–cholestric transition; they discussed the possibility of an enhanced sound attenuation in terms of domain scattering losses and *extremely weak* coupling between the orientational fluctuations and the sound wave. Rose and Shen[32] discussed the possibility of sound attenuation by scattering from cholestric domains. Such scattering would also lead to an exponential decay of the sound intensity[22] as long as the scatterers were independent.

The specific volume at the nematic–cholestric transition of PBLG–EDC[21] behaves in the same manner as the specific volume of PE6600 around T_u. Specific volume data for sufficiently high temperatures were not available in the literature and thus comparison could not be made with our data (*Figure 3d*). However, recent measurements on n-alkanes support the existence of a rather sharp bend at high temperatures[33].

The kinematic viscosity of TC and HTC clearly reflect a simple activated process above and below T_u thus following an exponential relationship (*Figure 4b*). The kinematic viscosity η^* is related to the dynamic viscosity η by:

$$\eta^* = \eta/\rho = \eta\{\rho(T_u)[1 - \alpha'(T - T_u)]\}^{-1} \tag{10}$$

To a first approximation, the temperature-dependent part of the density can be neglected, the error introduced by doing this is less than 10% for $T \leqslant 100$K.

$$\eta^* = B \exp\left(\frac{E}{kT}\right) \Big/ \left[\rho(T_u)\right] \tag{11}$$

The viscous behaviour below and above T_u may then be described by the following relationships for i = I,II [I, $(T < T_u)$; II, $(T > T_u)$]:

$$\ln(\eta_i^*) = \ln\left[\frac{B_i}{\rho(T_u)}\right] + \frac{E_i}{kT} \tag{12}$$

$$T_u = (E_{II} - E_I)/[k \ln(B_I/B_{II})] \tag{13}$$

The activation energies E_I and E_{II}, as well as temperature-independent pre-exponential terms B_I and B_{II}, are dependent upon molecular weight for a macromolecular system. If a potential law for E_I and E_{II} holds, we have:

$$E_i = E_{oi} \bar{M}_w^p \tag{14}$$

The B_i are assumed to be of the form $B_i = B_{oi} f(\bar{M}_w)$ with $f(\bar{M}_w) > 0$ at least over a limited range of $\bar{M}_w$[15]. Equation 13 then transforms to:

$$T_u = \bar{M}_w^p (E_{oII} - E_{oI})/[k \ln(B_{oI}/B_{oII})] \tag{15}$$

Taking values for T_u and $\bar{M}_w$ of TC and PE6600 the exponent p = 0.09 was determined from equation (14). From equation (15) and the values of activation energy for TC (*Table 1*) the parameters E_{oI} = 9.81 kJ mol^{-1} and E_{oII} = 8.1 kJ mol^{-1} can also be determined. Within the limits of the simple model described above the transition temperature T_u and the activation energies for viscous flow have been determined for high density polyethylene ($\bar{M}_w \sim 10^5$) below and above T_u:

$$T_u = 371°\text{C}$$

$$E_I = 27.9 \text{ kJ mol}^{-1}$$

$$E_{II} = 23.0 \text{ kJ mol}^{-1}$$

E_I is in fairly good agreement with the values of 25 and 27 kJ mol^{-1} found in literature[15]. The high value of T_u = 371°C explains why such a transition is unlikely to be found.

The viscous behaviour of $C_{36}H_{74}$ also shows a kink in the $\ln[\eta^*(1/T)]$ curve (*Figure 4b*). T_u was found to be at

123.5°C. This value is in good agreement with the extrapolated value (T_u = 124.2°C, equation 15).

The hypersonic behaviour of the amorphous PA6-3-T and PS is less homogeneous. Above the glass transition PA6-3-T shows no further kink in the sound velocity–temperature curve (*Figure 5*). Should there by any transition, this would be above 310°C. The sound attenuation has a maximum about T = 250°C and probably indicates the so-called 'high frequency glass transition'.

PS behaves similarly to partly crystalline polymers in sound velocity experiments, exhibiting a kink at T = 273°C. The hypersonic attenuation, however, behaves differently.

At this time, therefore, it is not clear whether there is a fundamental difference between crystallizing and non-crystallizing polymers with respect to the formation of an intermediate local nematic phase.

Fischer *et al.*[25] have discussed a hypothetical nematic–isotropic transition in n-alkanes far below the melt transition, in an attempt to explain their depolarized Rayleigh scattering data, magnetic birefringence measurements, etc. This conflicts with our interpretation of T_u. The ultrasonic data discussed above show that Brillouin scattering data should not mirror such a transition by critical softening or hardening of a phonon. The elastic behaviour found around T_u is not connected with a transition far below the melting temperature of paraffins.

Studies using other experimental techniques will be undertaken using other polymers to elucidate the remaining questions and problems.

ACKNOWLEDGEMENTS

The authors acknowledge fruitful discussions with Professor Dr H. -G. Unruh and Professor Dr E. W. Fischer. The authors express their thanks to A. Engelke, M. P. Boulard, A. Marx, H. Bastian and Dr G. I. Asbach for their help with some of the measurements and numerical evaluations.

This work was kindly supported by the Deutsche Forschungsgemeinschaft.

REFERENCES

1 Krüger, J. K. *Solid State Commun.* 1979, **30**, 43
2 Baltá Calleya, Berling, K. D., Cacković, H., Hosemann, R. and Loboda-Cacković, J. *Macromol. Sci. (B)* 1976, **12**, 383
3 Rehwald, W. *Adv. Phys.* 1973, **22**, 721
4 Unruh, H. -G., Krüger, J. K. and Sailer, E. *Ferroelectrics* 1978, **20**, 3
5 Krüger, J. K., Peetz, L. and Pietralla, M. *Polymer* 1978, **19**, 1397
6 Pechold, W. and Blasenbtey, S. *Kolloid. Z. Polym.* 1970, **241**, 955
7 Yeh, G. S. Y. *J. Macromol. Sci. (B)* 1972, **6**, 465
8 Geil, P. H. in G. Allen, S. E. B. Petrie (Eds.)
9 Boyer, R. F. 'Physical structure of the amorphous state', Marcel Dekker, New York, 1976
10 Mitsui Petrochemical Ind. Ltd., Technical Report
11 Schneider, J. *Kunststoffe* 1974, **64**, 1
12 May, W., Kiefte, H., Clauter, M. J. and Stegemann, G. J. *Appl. Optics* 1978, **17**, 1603
13 Krüger, J. K., Pietralla, M. and Bastian, H. to be published
14 'Polymer Handbook', 2nd Edn, (Eds. J. Brandrup and E. H. Immergut) Wiley, New York, 1975
15 van Krevelen, D. W. 'Properties of Polymers' Elsevier, Amsterdam, 1976, p 331
16 Brody, E. M., Lubell, C. J. and Beatty, C. L. *J. Polym. Sci. (Polym. Phys. Edn)* 1975, **13**, 295
17 Coakley, R. W., Mitchell, R. S., Stevens, J. R. and Hunt, J. L. *J. Appl. Phys.* 1976, **47**, 4271
18 Patterson, G. D. *J. Polym. Sci. (Polym. Phys. Edn)* 1977, **15**, 579
19 Blasenbrey, S., Pechold, W. *Ber. Bunsengesellschaft* 1970, **74**, 785
20 de Gennes, P. G. 'Physics of Liquid Crystals', Clarendon Press, Oxford, 1974
21 Uematsu, J. and Uematsu, I. in 'Mesomorphic Order in Polymers and Polymerization in Liquid Crystalline Media' (Ed. A. Blumstein) Am. Chem. Soc. 1978, Washington
22 Truell, R., Elbaum, C. and Chick, B. B. 'Ultrasonic Methods in Solid State Physics', Academic Press, New York, 1969
23 Wallis, W. A. and Moore, G. M. *J. Am. Statist. Assoc.* 1971, **36**, 401
24 Krüger, J. K., Schollmeyer, E. and Barthel, J. *Z. Naturforsch.* 1975, **30a**, 1476
25 Fischer, E. W., Strobl, G. R., Dettenmaier, M., Stamm, M. and Steidle, N. submitted to *Discuss. Faraday Soc.* Preprint No. 296, 1979
26 Lemaire, B. and Botherel, P. *J. Polym. Sci. (Polym. Lett. Edn)* 1978, **16**, 321
27 Eden, D., Garland, C. W. and Williamson, R. C. *J. Chem. Phys.* 1973, **58**, 1861
28 Nagai, S., Martinoty, P. and Canadau, S. *J. de Phys.* 1976, **37**, 769
29 Kozhevnikov, E. N. and Chaban, I. A. *Akust. Zh.* 1978, **24**, 363
30 Durand, G. and Narasimha Rao, D. V. G. L. *Phys. Lett.* 1968, **27A**, 455
31 Wang, C. H. and Huang, Y. Y. *J. Chem. Phys.* 1975, **62**, 3834
32 Rosen, H. and Shen, Y. R. *Mol. Cryst. Liquid Cryst.* 1972, **18**, 285
33 Grossmann, H. P. unpublished results